Hindawi Publishing Corporation
Shock and Vibration
Volume 2014, Article ID 295279, 12 pages
http://dx.doi.org/10.1155/2014/295279

Research Article

Multiple-Echo Suppression Modeling and Experimental Verification for Acoustic Transmission along Periodic Drillstring Using Dual Receivers

Li Cheng,[1,2] Chang Jinfeng,[1,2] Liu Zhao,[1,2] and Fan Shangchun[1,2]

[1]*State Key Laboratory of Virtual Reality Technology and System, Beihang University, Beijing 100191, China*
[2]*Science and Technology on Inertial Laboratory, Beihang University, Beijing 100191, China*

Correspondence should be addressed to Li Cheng; lc.bj@163.com

Received 10 July 2014; Revised 23 September 2014; Accepted 8 October 2014; Published 31 December 2014

Academic Editor: Chao Tao

In the oil industry, the accompanied reverberation is a major constraint in the transmission rate and distance because the drillstring is a heterogeneous assembly. Based on the transient impulse responses in uplink and downlink channels, an improved simplified echo suppression model with two acoustic receivers is presented in consideration of position optimization of single acoustic receiver. Then the acoustic receiving characteristics of transmitted signals in a length-limited periodic drillstring channel are obtained in single- and dual-receiver modes. An additive downward white Gaussian noise is also introduced in the channel. Moreover, an experimental rig is established by using a rotatable electromagnetic vibration exciter and two piezoelectric accelerometers, which are spaced one-quarter wavelength apart along a 6.3-meter simulated periodic drillstring. The ASK-, FSK-, and PSK-modulated square-wave pulse sequences at a transmission rate of 200 bit/s are applied to the simulated drillstring at a rotation speed of 0, 80, and 140 r/min, respectively. The experimental results show that the dual-receiver mode can exhibit a significantly improved average error bit ratio, which is approximately 2.5 to 3 times lower than that of the single-receiver mode, especially under the conditions of higher rotation speeds.

1. Introduction

In the exploration industry, there is a need for some means of transmitting downhole drilling information, such as pressure, temperature, drilling direction, and formation information, to the surface [1, 2]. With the development of electronic circuits and digital signal processing technologies, many downhole measurement tools in measurement while drilling (MWD) are developed to collect the downhole information [3]. The various downhole telemetry methods have been attempted, including mud pulse telemetry, high-speed drillstring telemetry, wireline telemetry, extremely low frequency electromagnetic (EM) telemetry, and drillstring acoustic telemetry. The mud pulse telemetry is the most commercially successful method. However, the data transmission rate is limited to a few bits per second due to attenuations and spreading of pulses. When highly compressible underbalanced drilling fluid is used, such an approach may fail to work [4]. High-speed drillstring telemetry can be implemented by using a unique system of wired drill pipes and associated drilling tools connecting the MWD string to the surface [5]. Because special drill pipes and special tool joint connectors are required, the cost of the drilling operation will be substantially increased. In wireline telemetry, the measured parameters are converted into electrical signals and transmitted through a coaxial cable. However, it is improper to use the electrical cable during drilling because either electrical connections are required every 10–15 m or the drilling has to stop for the cable to be tripped out in order to add a new pipe segment. Moreover, the available space outside the tubing is confined and the cable can easily be damaged [6]. As a result, wireless telemetry systems are preferred in such measurement during drilling operations. At present, EM telemetry has been used for MWD services, but EM signals encounter high attenuation in regions of low formation resistivity. Especially the data rate and transmission range are limited

by the resistivity of the formation surrounding the borehole [7]. Acoustic data transmission along the drillstring via extensional waves offers another communication possibility. The idea of acoustic wave transmission through the drillstring was initially proposed in 1948 by Sun Oil Company, which also performed a field test to measure acoustic attenuation in a drillstring and reported a signal loss of about 12 dB/1000 ft [8]. Unfortunately, the drillstring is a periodic structure of pipes and threaded tool joints, thereby featuring a banded and dispersive behavior. Although a multinode acoustic telemetry network capable of transmitting data at over 30 bits per second has been developed and successfully deployed in drilling application, the transmitted acoustic data are disturbed by short- and long-period reverberations caused by the multiple reflections in the drillstring [9]. These physical constraints strongly deteriorate the signal-to-noise ratio (SNR), thereby restraining seriously the available transmission distance and data rate for this type of acoustic telemetry. Hence, the echo suppression is a more critical problem at multiple acoustic impedance mismatch positions, where echoes travel freely up and down the drillstring and confuse the transmission data.

In recent years, some new developments in echo cancellation have been described in telecommunications, more particularly in mobile communications [10–12]. These echo cancellers mainly use adaptive filters to combat the interference of the transmitted signal on the collocated receivers in order to accomplish full-duplex transmission over networks. The echo path includes a delay, which basically consists of a system-delay component and a propagation time from loudspeaker to microphone. However, it will degrade the convergence speed and the performance due to overparameterization. Computational complexity is also a major issue in delay estimation, which may even make the algorithm infeasible to implement in a real-time system. Consequently, a simplified echo suppression algorithm is more preferable for acoustic transmission along the drillstring in real time under adverse downhole conditions. Besides, the term "echo" represents the transmission of the signal back to the transmitter in mobile communications [13], while the echo disturbs the receiving of the transmitted signal at the receiver in downhole acoustic communications. With regard to the problems above, Rector and Marion used a data-dependent deconvolution operator to perform the inverse filtering of the multiple acoustic reflections [14]. The main disadvantage is that it may induce signal distortion due to coherent noise. Drumheller and Scott demonstrated an echo suppression method of using a novel digital time delay circuit and a pair of spaced sensors, such as strain gages or accelerometers, to perform the echo suppression [15]. However, the exact time delay of travelling waves between the two sensors and adaptive filters needs to be determined. Poletto presented a dual-sensor-based reverberation suppression analysis method by measuring acceleration and strain with opposite reflection coefficients [16]. Addition of the dual waves makes it possible to remove part of the drillstring reflections, whereas it is more prone to reduce the one-way reflection noise from one end of drillstring. Considering that the surface noise is a dominant noise source, Sinanović et al. presented a theoretical two-receiver channel model [17]. In this model, different time delays between the two signals at two receivers are used to suppress the surface noise. However, the model only takes into account first-order wave reflections at the pipe ends for simplicity. As a matter of fact, acoustic reflections occur not only at pipe ends, but also at any acoustic impedance mismatch positions in drillstring. Thus it will fail to work in an actual operation due to the oversimplified solutions when multiple reflections are considered. In this paper, an improved multiple-echo suppression model using two acoustic receivers is proposed based on the transient pulse responses in uplink and downlink channels. And an experimental rig for imposing the vibration excitation on a rotary simulated drillstring is established to examine acoustic data transmission behaviors. The acoustic receiving characteristics of transmitted signals, including unit sinusoidal pulse sequences and square-wave modulation data, along the simulated drillstring are investigated in single- and dual-receiver modes by simulation and experiment, respectively.

2. Model Adapted to the Problem

The drillstring acoustic telemetry method has been studied in the foregoing papers [18]. Barnes and Kirkwood in 1972 have indicated that the periodic structure formed by the pipes and the tool joints results in frequency filtering and multiple echoes [19]. Acoustic impedance mismatches produced by discontinuous structure of drillstring also manifest surface and downhole noises through numerous spikes within each of the passbands of the transmission spectrum. The results of this analysis illustrate the importance of suppressing echo noises and enhancing the upward travelling acoustic telemetry signal collected by receivers. In this section, acoustic transmission performance along a finite-length drillstring is simulated by a time-domain finite-difference method using the following equation:

$$\frac{\partial^2 u}{\partial t^2} = \frac{E}{\rho}\frac{\partial^2 u}{\partial x^2}, \tag{1}$$

where E, ρ, u, and A are the Young's modulus, density, longitudinal displacement, and cross-sectional area of drillstring, respectively. In view of the fact that the periodic structure will cause a redistribution and not merely a reduction of amplitude and spreading of the wave, attenuation mechanisms in the actual field environment, including viscous dissipation of energy into the surrounding drill mud and physical contact with the formation and well casing, are not included in (1).

By introducing the mass coordinate m and the acoustic impedance z, (1) is rewritten as

$$\frac{\partial^2 u}{\partial t^2} = \frac{\partial}{\partial m}\left(z^2\frac{\partial u}{\partial m}\right), \tag{2}$$

where c is the sound speed in the drillstring and the acoustic impedance $z = \rho Ac$.

The time-domain algorithms of linear, one-dimensional wave equations have the advantages for many problems with complex combinations of geometry and boundary conditions. The drillstring is divided into the segments. Within

each segment, it is assumed that the density and the cross-sectional area are constant. The position of mesh point x_n is labeled with an integer n. The position within the segment between meshes points x_n and x_{n+1} is labeled with a number $n + 1/2$. The displacement field $u(x,t)$ at the mesh point x_n is approximated by a discrete set of values u_n^j. In order to improve the stability of the algorithm, uniform critical time step Δt and mass element Δm are used. And Δm is defined as $\rho Ac\Delta t$ for a uniform drillstring element. By using a simple-centered difference method, (2) is given by

$$u_n^{j+1} = \frac{z_{n+1/2}\left(2u_{n+1}^j - u_n^{j-1}\right) + z_{n-1/2}\left(2u_{n-1}^j - u_n^{j-1}\right)}{z_{n+1/2} + z_{n-1/2}}, \quad (3)$$

where j denotes the time $j\Delta t$; Δt is critical time step; n denotes the position x_n. By specifying the boundary conditions

$$\begin{aligned} u_n^j &\quad (j = 0, 1;\ n = 0, 1, 2, \ldots, N), \\ u_n^j &\quad (j = 0, 1, 2, \ldots, N;\ n = 0, N), \end{aligned} \quad (4)$$

acoustic transmission transient behaviors along the drillstring can be analyzed.

2.1. Acoustic Receiver Position in Drillstring. In acoustic telemetry, the characteristic impedance is a function of frequency and position, the position dependence being periodic in accordance with the period of a drillstring. Therefore, the received signal is affected by the positions of transceivers in the drillstring. The transmitted signal travels in both directions through the drillstring. For simplicity, the first-order reflection at the top end is only considered in (5), but the results generalize when multiple reflections are taken into account. Assuming the upward transmitted signal from the bottom end is $y_2 = A\cos\omega(t - L_u/v)$, the received signal is given by

$$\begin{aligned} y &= A\cos\omega\left(t - \frac{L_u}{v} + \frac{L}{v}\right) - A\cos\omega\left(t + \frac{L_u}{v} + \frac{L}{v}\right) \\ &= 2A\sin\omega\left(t + \frac{L}{v}\right)\sin\frac{2\pi L_u}{\lambda}, \end{aligned} \quad (5)$$

where L_u is the distance of the receiver relative to the top end; λ is the wavelength; L is the distance between transmitter and receiver; v is the wave speed.

From (5), the preferred placement L_u of acoustic receiver can be defined as $n\lambda/4$ by the maximum value of y, where n is any odd integer greater than zero. However, the upper end of drillstring is more closely modeled as a fixed end rather than a free end due to the mass of the blocks suspending the drillstring or the mass of the drilling platform. The receiver may also be located near the end of drillstring. As a result, the preferred location for a single acoustic receiver is near the end of drillstring or at the position of approximately $n\lambda/4$ below the upper end to minimize destructive interferences by signal reflections [20]. Assuming the drillstring is composed of nine drill pipes, which are separated by eight tool joints. According to the passband and stopand frequency response of drillstring, the carrier frequency is set as 1455 Hz. The end of drillstring at the side of the receiver is regarded as a fixing end. Then the transient channel response to an excitation signal, composed of ten sine wave pulses, can be obtained by the finite-difference method. The drillstring physical dimensions in simulation are listed in Table 1.

Table 1: Drillstring dimensions.

	Cross-sectional area (m^2)	Length (m)
Drill pipe	3.39×10^{-3}	9.11
Tool joint	16.2×10^{-3}	0.475

Figure 1 compares the received signals at the position of $\lambda/4$ away from the top end with those at the position of λ away from the top end. The aliasing of the direct waves and the reflective waves at the position of $\lambda/4$ produces less peaked noise, while the reflection interferes destructively with the original signals at the position of λ in Figure 1(a). Moreover, the signal intensity in frequency domain response at the position of $\lambda/4$ is twice stronger than that at the position of λ in Figure 1(b), which contributes to the increase of SNR and transmission performance, such as transmission rate and distance. Thus, it is more appropriate to place an accelerometer at a distance of $\lambda/4$ down from the top end to detect the upward travelling waves in a single-receiver mode.

2.2. Dual Acoustic Receiver Model in Drillstring. During the drilling, both bit noise and surface noise seriously confuse the transmission of data. When the two types of noises are assumed to be additive and Gaussian, the dominant noise component in the channel capacity is the surface noise for a given bandwidth [17]. Thus the bit noise is commonly ignored for simplicity. Unfortunately, acoustic telemetry signals are usually disturbed by multiple reverberations produced by the reflections occurring at acoustic impedance mismatch positions. Dual measurements record the reflected waves travelling in the same direction and make it possible to remove the reflections of drillstring waves and unwanted noises.

Referring to Figure 2, the acoustic receivers S_1 and S_2 spaced one-quarter wavelength apart are placed on the first pipe at the top of drillstring to record the signals, $n_s(t)$ and $x(t)$, and their reflections. The noise $n_s(t)$ consists of the direct surface noise as well as the downlink echoes of mixed signals from the direct surface noise and the original excitation signal $x(t)$. Based on the standing wave theory, the receiver S_1 is located approximately near the top end of drillstring, and the lower receiver S_2 is $\lambda/4$ away from the receiver S_1. Due to the presence of multiple reflections in the drillstring channel, the uplink and downlink channel responses are introduced in the proposed model. Assuming that a unit pulse excitation is imparted on the bottom end of drillstring, the pulse excitation responses obtained by the receivers S_1 and S_2 are defined as $h_1(t)$ and $h_2(t)$, respectively. Similarly, assuming that a unit pulse excitation is imparted on the top end of drillstring, the pulse excitation responses collected by the two receivers are defined as $h_1'(t)$ and $h_2'(t)$,

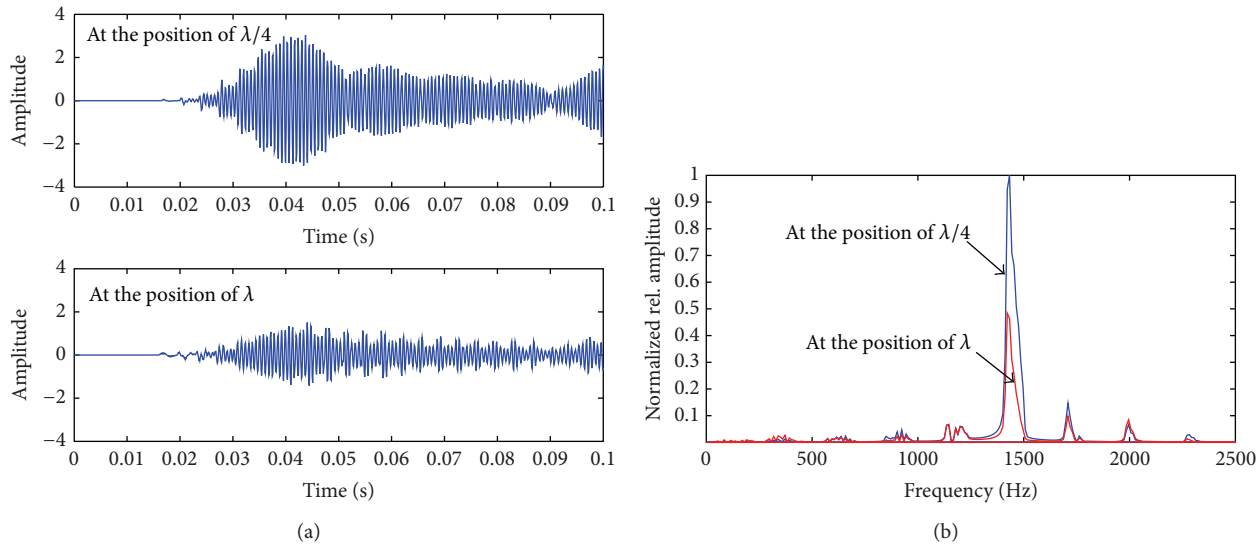

Figure 1: Simulation results of received signals at different receiving positions. (a) Time-domain signal, (b) frequency-domain signal.

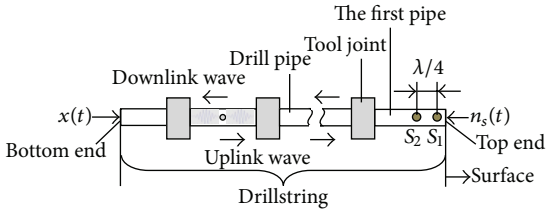

Figure 2: Schematic diagram of the proposed model.

respectively. In terms of the channel model in Figure 2 [21], the resulting signals y_1 and y_2 at the receivers S_1 and S_2 are

$$y_1(t) = x(t) * h_1(t) + n_s(t) * h_1'(t),$$
$$y_2(t) = x(t) * h_2(t) + n_s(t) * h_2'(t). \quad (6)$$

By a fast Fourier transform (FFT) algorithm, (6) are written as

$$Y_1(f) = H_{X_1}(f) X(f) + H_{N_1}(f) N_s(f),$$
$$Y_2(f) = H_{X_2}(f) X(f) + H_{N_2}(f) N_s(f), \quad (7)$$

where $H_{X_1}(f)$, $H_{X_2}(f)$, $H_{N_1}(f)$, and $H_{N_2}(f)$ represent the functions of $h_1(t)$, $h_2(t)$, $h_1'(t)$, and $h_2'(t)$ in the frequency domain, respectively.

Since the downward moving noise $n_s(t)$ disturbing acoustic signal extraction is a mixture of the noise and data along with multiple reflection waves, the following result can be achieved by (7) to minimize the amount of noise being transmitted upward towards the surface. Consider

$$X(f) = \frac{H_{N_2}(f) Y_1(f) - H_{N_1}(f) Y_2(f)}{H_{X_1}(f) H_{N_2}(f) - H_{X_2}(f) H_{N_1}(f)}. \quad (8)$$

With inverse Fourier transform, the original excitation signal $x(t)$ can be computed by

$$x(t) = F^{-1}\left(\frac{H_{N_2}(f) Y_1(f) - H_{N_1}(f) Y_2(f)}{H_{X_1}(f) H_{N_2}(f) - H_{X_2}(f) H_{N_1}(f)}\right). \quad (9)$$

The recovered signal $x(t)$ detected by dual receivers will be processed with a bandpass filter so that the carrier frequency is limited to the passbands for data transmission. And it can eliminate the high-frequency components introduced by the algorithm. Especially, it is important to note that the uplink and downlink channel responses $h_1(t)$, $h_2(t)$ and $h_1'(t)$, $h_2'(t)$ at the two receivers S_1 and S_2 can be measured, respectively. The two receivers can be piezoelectric or magnetostrictive accelerometers in real applications. The corresponding uplink and downlink channel responses are firstly sampled after a known chirp signal is generated at the downhole transmitter and the surface location of drillstring. Then the channel transfer function may be determined by cross-correlating the received signal with the reference chirp signal, using a frequency spectrum of the received signal and a frequency spectrum of the reference chirp signal. Thus the functions $H_{X_1}(f)$, $H_{X_2}(f)$, $H_{N_1}(f)$, and $H_{N_2}(f)$ in (8) may be eventually solved. The original excitation signal $x(t)$ can be intercepted and recovered from (9).

3. Simulation of Acoustic Transmission Using Dual Receivers

Four drill pipes are separated by three tool joints as listed in Table 1, which are used in the transient simulation. The whole length of studied drillstring is about 37.8 m. From the classical patterns of passbands and stopbands in the wave spectra, the carrier wave of 1.52 kHz frequency in the passbands is determined. Referring back to Figure 2, a continuous sine or modulated excitation signal is applied at the left end. The receiver S_1 is located 0.95 m away from the right end, and

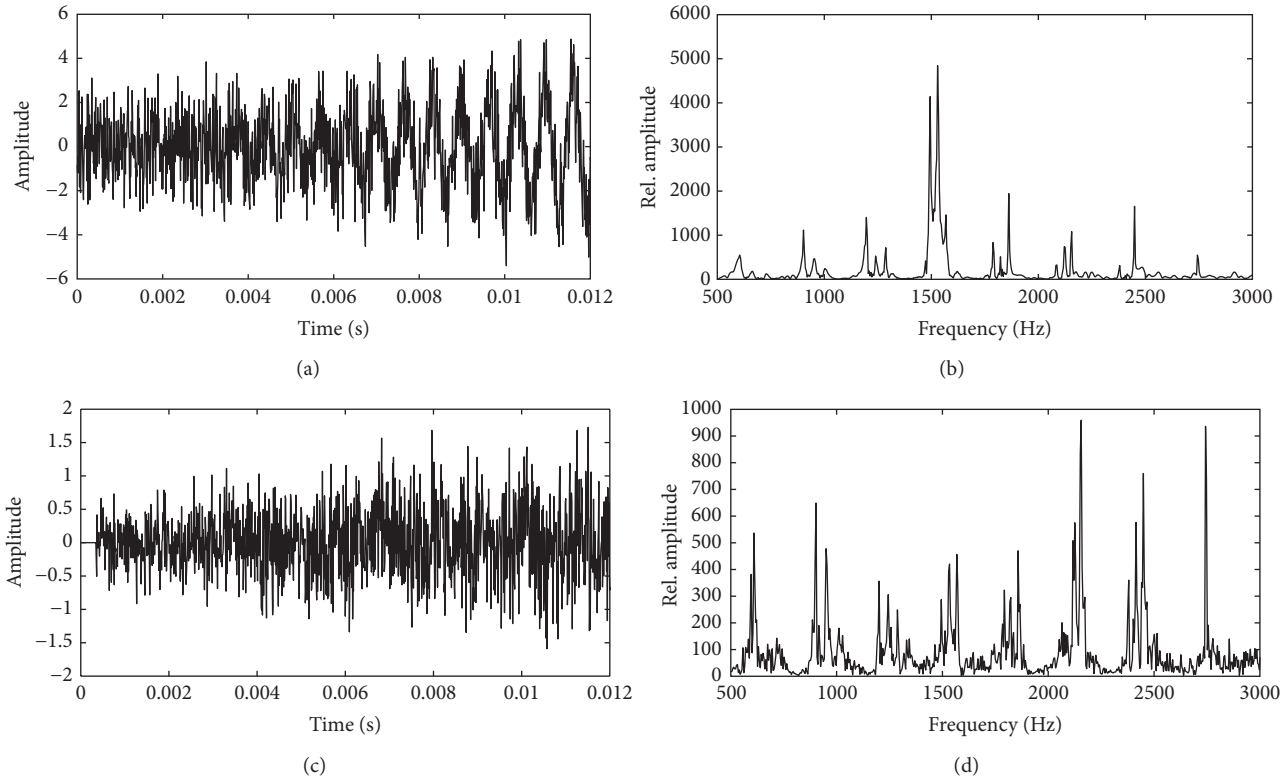

FIGURE 3: Simulation results of received signals in the single-receiver mode. (a) Time-domain waveform at the receiver S_1, (b) frequency-domain waveform at the receiver S_1, (c) time-domain waveform at the receiver S_2, and (d) frequency-domain waveform at the receiver S_2.

the receiver S_2 is at 0.95 m below the receiver S_1. The left and right ends are, respectively, regarded as the bottom and top ends of drillstring, wherein the right end is modeled as a fixed end because of the mass of the blocks suspending the drillstring or the mass of the drilling platform. An additive white Gaussian noise with a SNR of 4 dB is acted on the right end, which simulates the effect of downward surface noise. By solving the transient responses to unit pulse excitation at the receivers S_1 and S_2 in uplink and downlink channels in the form of one-dimensional wave equation, the functions $h_1(t)$, $h_2(t)$, $h_1'(t)$, and $h_2'(t)$ in (6) are confirmed. In this way, the original excitation signal $x(t)$ is available to be extracted with the foregoing dual-receiver method.

3.1. Sine Pulse Excitation. A packet of fourteen oscillations of 1.52 kHz is acted on the left end of drillstring. The receivers S_1 and S_2 simultaneously detect the transient wave motions. Then the achieved signals in single- and dual-receiver modes are compared as shown in Figures 3 and 4. The received signal at the receiver S_2 is heavily attenuated and distorted with stronger high-frequency interference components, such as 2.15 kHz and 2.86 kHz far away from the 1.52 kHz excitation frequency in Figure 3(b). The corresponding time-domain signal has lost the original pulse shape, which may result from the worse receiving position of 1.9 m (approximately $\lambda/2$) away from the right end. On the contrary, the center frequency of the signal at the receiver S_1 is coincident with the transmitted frequency of 1.52 kHz in Figure 3(a). In Figure 4, the dual-receiver signal has smoother sine-wave shapes and fewer resonant peaks, although its amplitude falls in between those of signals received by the receivers S_1 and S_2. This also indicates to a certain extent that a single receiver inserted near these optimal positions is feasible under higher SNR conditions. On account of the burrs superimposed with much interference signals, a 60-order bandpass finite impulse response (FIR) filter (1400–1620 Hz) using Hamming window is applied in the dual-receiver mode. The filtered waveform is shown in Figure 5. By comparing Figure 4 with Figure 5, the burrs and high-frequency peaks are by far removed in the filtered signals. From the obtained well-behaved signal envelope, we conclude that the established dual-receiver model can make it possible toimplement echo cancellation and noise reduction under lower SNR conditions.

3.2. Modulated Signal Excitation. The assembled drillstring has periodically spaced discontinuities in cross-sectional area. It has been discovered that certain discrete frequency passbands exist in a drillstring, which permits the transmission of an acoustic signal with a minimum level of attenuation. Thus it is essential for the signal modulation to make the frequency range of transmitted signals within an optimum passband. The binary data is generally transmitted in one of three basic ways, such as amplitude-shift keying (ASK) modulation, frequency-shift keying (FSK) modulation, and phase-shift keying (PSK) modulation [22]. And currently simple communication modulation schemes, such as ASK,

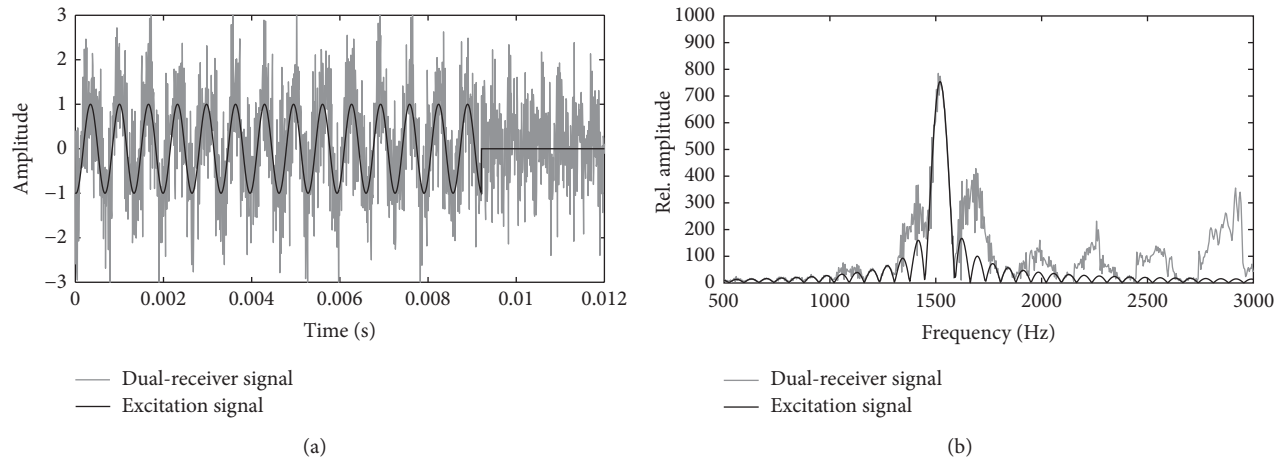

Figure 4: Simulation results of received signal in the dual-receiver mode. (a) Time-domain waveform, (b) frequency-domain waveform.

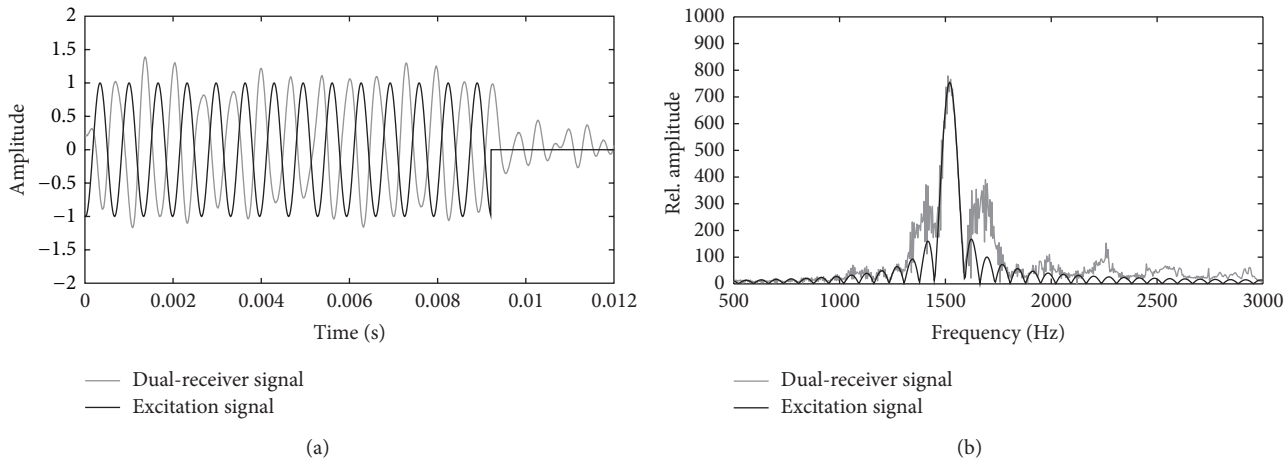

Figure 5: Simulation results of filtered signals in the dual-receiver mode. (a) Time-domain waveform, (b) frequency-domain waveform.

FSK, PSK, and their derivatives, are still commonly applied to actual downhole telemetry systems. Therefore, from the view of the principle experiment and the performance test, the three classic digital communication modulation schemes are employed to evaluate the proposed dual-receiver method. A packet of 50-bit modulated pseudorandom binary code sequence, which comprises a series of ones and zeros in a seemly random pattern known to both the transmitter and receiver, is brought to bear on the left end of drillstring. The carrier frequency and data rate are configured to be 1.52 kHz and 450 bit/s, respectively. An additive white Gaussian noise with zero mean and a variation of 8 is acted on the top end of drillstring to simulate the effect of downward-going surface noise $n_s(t)$. In this case, the mixed signal and noise coexist in the periodic fading simulation channel. The output of the receiver S_1 at the optimal position is recommended as a single receiver signal. Each of digital modulation schemes is tested by simulation for twenty times to evaluate the performance of acoustic data communication. Then the bit error rate (BER) curves along a 37.8-meter drillstring for the three different types of modulation in either single- or dual-receiver mode are presented in Figure 6. The simulation results show that the there is no obvious difference in the average BER with the range of 47%–50.4% for the three types of modulation in single-receiver mode, while the average BER is significantly improved and reduced by more than 94% when the dual-receiver mode is available. In general, the PSK modulation is less susceptible to errors than the other two modulation schemes in nonrotary drillstring channel, while it requires more complex phase recovery process. Specifically, the average BER of PSK-modulated pulse signal is reduced by up to 0.8% from 47% when the dual-receiver prototype is substituted for single-receiver prototype. The corresponding transmitted and received waveforms of PSK-modulated signal are demonstrated in Figure 7. It turns out that the appropriate use of two receivers with a proper modulation scheme can offer a better SNR and a higher data rate in multipath channel of drillstring.

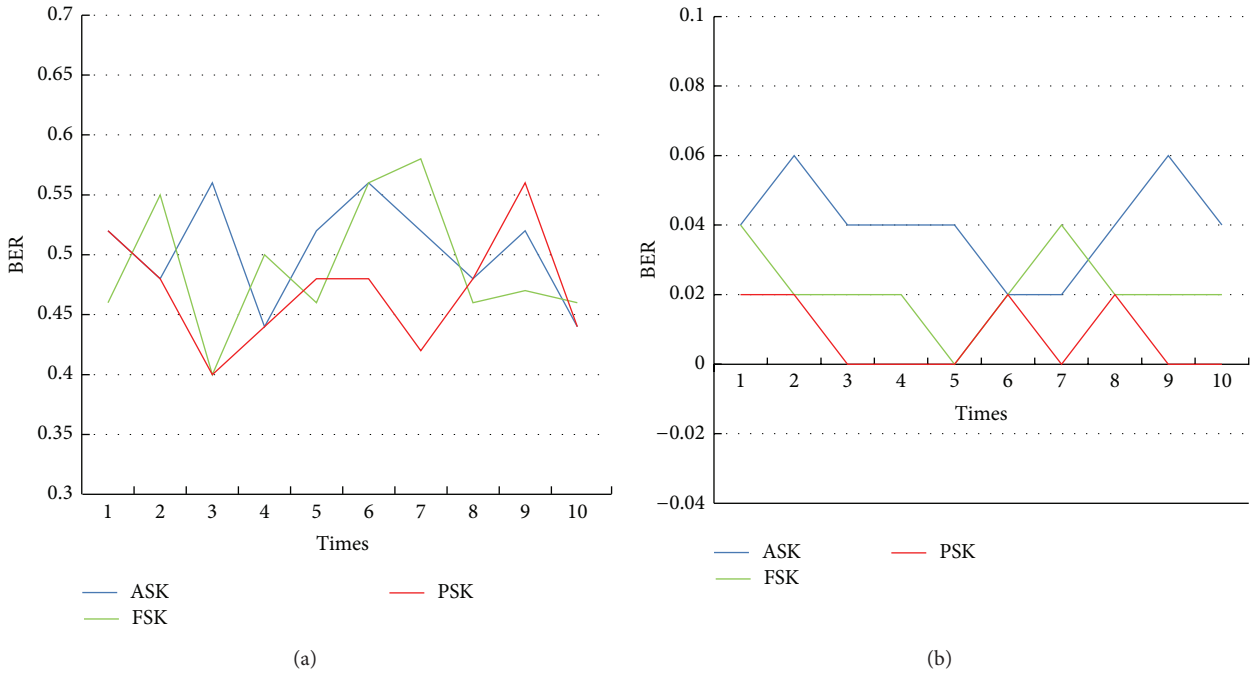

FIGURE 6: The BER simulation curves of ASK-, FSK-, and PSK-modulated data in the single- and dual-receiver modes. (a) Single-receiver mode, (b) dual-receiver mode.

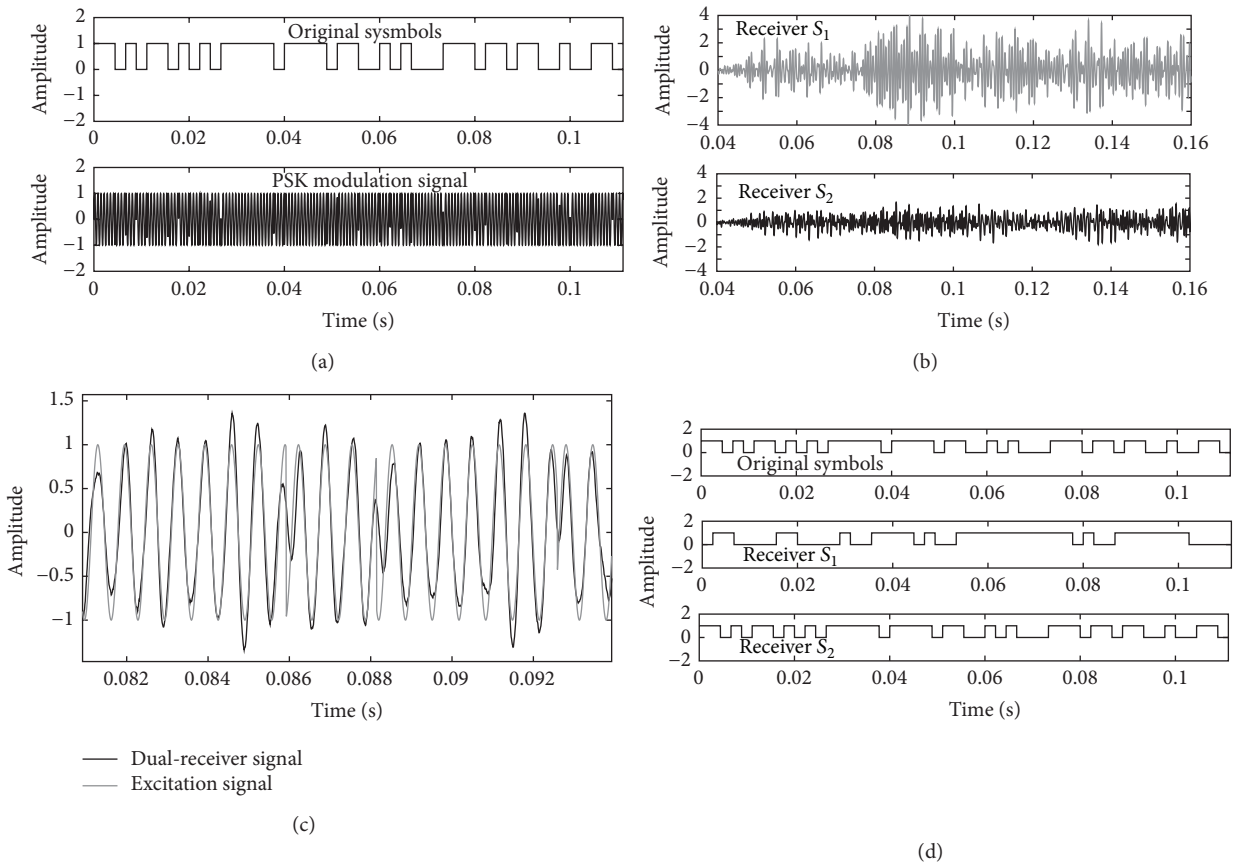

FIGURE 7: Simulation results of transmitted and received PSK-modulated data. (a) Excitation signal, (b) received signal at the receivers S_1 and S_2, (c) magnification of dual-receiver signal, and (d) recovered binary data.

Table 2: Dimensions of simulated drillstring.

	Cross-sectional area (m^2)	Length (m)
Circular pipe	0.75×10^{-3}	1.5
Tool joint	1.13×10^{-3}	0.1

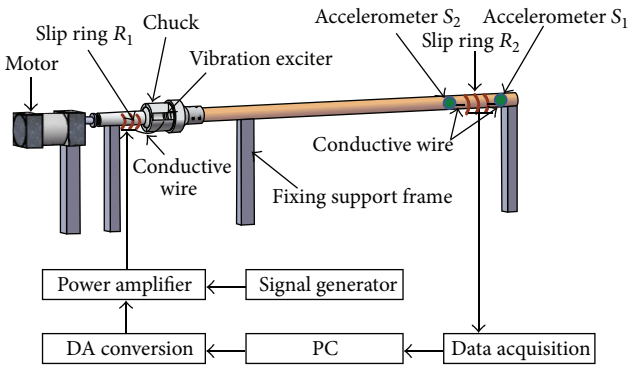

Figure 8: Schematic diagram of the established experimental rig.

4. Experimental Results and Analysis

Figure 8 illustrates a developed experimental rig to perform vibration acceleration measurement and acoustic data transmission along the simulated drillstring in the laboratory. According to the analogical principle, a set of circular pipes are adopted to construct the simulated periodic drillstring. The circular pipes made of 45# carbon steel are screwed end-to-end to simulate the actual drillstring by threaded tool joints. The whole length of the simulated drillstring, formed by four circular pipes and three tool joints, is approximately 6.3 m. The dimensions of the simulated drillstring are listed in Table 2.

The lower circular pipe on the left for the simulated drillstring is hinged with one end of a chuck. The other end of the chuck is connected with a short connecting shaft by a threaded pipe connection. The short shaft is driven by a motor which is supported by a fixing frame with a support base plate made of 45# carbon steel. An electromagnetic vibration exciter with a 10 N dynamic force output is mounted into the chuck by fixing bolts, which in this way is capable of allowing the exciter to exert a desired vibration excitation on the rotary simulated drillstring. The right end of the simulated drillstring is fastened to the fixing support frame such that the right end is regarded as a fixing end. Two single-axis integrated electronic piezoelectric (IEPE) accelerometers spaced at a spacing of $\lambda/4$ are used to measure the vibration responses to the excitation signal. The accelerometer S_1 is located $\lambda/4$ away from the right end of the simulated drillstring, and the accelerometer S_2 is on the left side of the accelerometer S_1. According to the arrangement in Figure 8, the output of the signal generator is imported to the vibration exciter via a power amplifier, and then the exciter can apply a corresponding dynamic force to the left end of simulated drillstring. The motor drives the simulated drillstring by a machined short shaft and makes it rotate at a certain rotation speed. As a result of the rotary excitation, the signal outputs

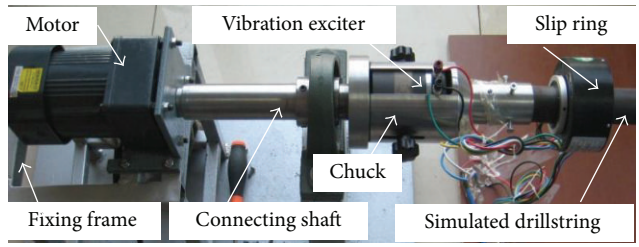

Figure 9: Physical picture of rotary vibration excitation device.

of used accelerometers are unable to connect to a computer-based data acquisition device using a direct cable connection. For this reason, two slip rings R_1 and R_2 are used to lead the current through stationary brushes into or out of a winding on the simulated drillstring. At the same time, they are available to perform the rotary vibration excitation and the rotary vibration measurement, respectively. The accelerometer signals received by the receivers S_1 and S_2 are fed to a four-channel data acquisition device YE6231 connected with a computer in real time, where the sampled time-domain vibration data are processed to recover the excitation signals. Figure 9 reveals the physical picture of the developed rotary vibration excitation device. The typical performance parameters of experimental devices are listed in Table 3.

It is important to notice that the impedances of the tool joints are about five times greater than the impedances of the pipes. The simulated drillstring also exhibits the classical characteristics that are similar to those of an electrical comb filter [23]. Thus the optimal passband and the carrier frequency should be assigned for acoustic data transmission. The channel response experiments are firstly performed by using an impact hammer. An impulse load is impacted on the simulated drillstring at the left end in the axial direction of pipes. Immediately after the impact in Figure 10(a), the resulting right-traveling wave is recorded by the uniaxial accelerometer S_1 at the position adjacent to the right end. The impulse response is shown in Figure 10(b). Because of the nonideal impact excitation and the coupled vibrations of slightly curved simulated drillstring, the measured response to the hammer impact excitation is different from the theoretical response. However, as shown in Figure 10(b), the frequency spectrum also predicts the alternative passbands and stopbands due to the periodic structure of simulated drillstring. The frequency regions, representing the passbands and the stopbands, are denoted by the symbols "P" and "S" in Figure 10(b), respectively. The amplitude of the signal in the stopbands is much lower. Moreover, the number of typical spikes within each passband is related to the number of drill pipes in the drillstring. Consequently, the preferable frequency of 1.5 kHz within the second passband is determined as the carrier frequency of modulated oscillation excitations by the hammer impact experiment.

Digital information is binary in nature in that it has only two possible states "1" or "0." Since a square wave contains abrupt amplitude shifts between two different values, it is a preferred method of transmitting digital data over short distances. Each bit is represented by a square-wave pulse

Table 3: Typical performance parameter of experimental devices.

Device	Model	Typical performance parameter
Vibration exciter	JZ-2A	Output force: 10 N; operation bandwidth: 10 Hz–18 kHz; maximum output displacement: ±3 mm
Power amplifier	GF-20	Maximum output voltage: 20 V; operation bandwidth: 5 Hz–20 kHz
IEPE accelerometer	CA-YD-186	Sensitivity: 100 mV/g; maximum acceleration allowed: 50 g; operation bandwidth: 0.5 Hz–5 kHz
Data acquisition device	YE6231	Resolution: 24 bit; sampling frequency: 96 kHz/Ch; signal input frequency: 0.3 Hz–30 kHz
Signal generator	RIGOL5102	Sampling rate: 1 GSa/s; maximum output frequency: 100 MHz; modulation type supported: AM, FM, PM, ASK, FSK, PSK, PWM, IQ
Motor	51K90RGN-CF	Rated power output: 90 W; maximum rotation speed: 200 r/min

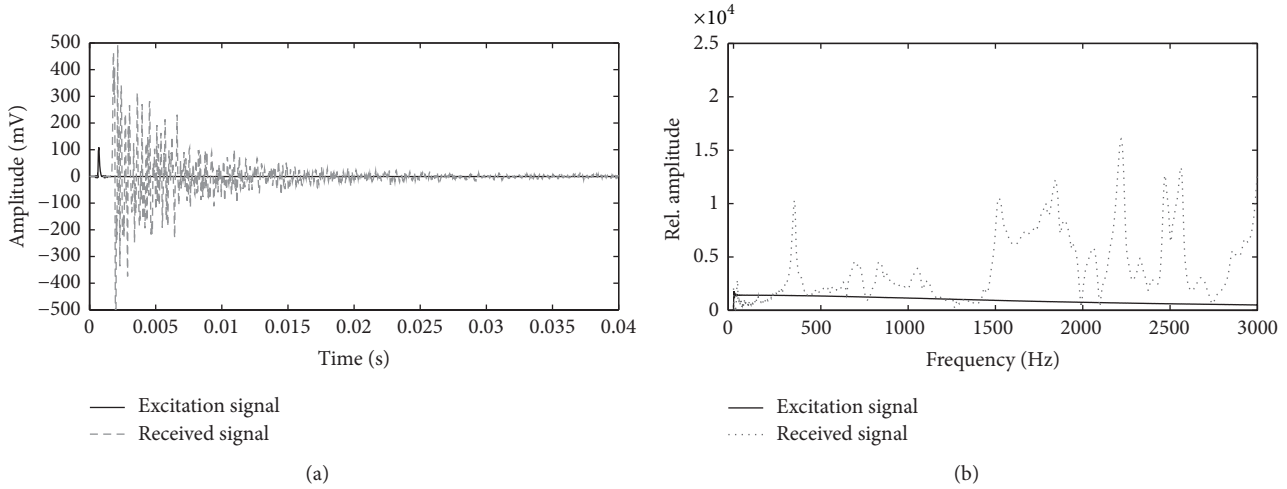

Figure 10: The measured hammer excitation and channel response signals. (a) Time-domain signal, (b) frequency-domain signal.

whose duration is predetermined by the baud bit. In consideration of used short 6.3-meter simulated drillstring in the laboratory, an ASK-, FSK-, or PSK-modulated square-wave pulse sequence produced by signal generator RIGOL 5102 is firstly operated by the power amplifier GF-20 and then imposed on the length-limited simulated drillstring by the assembled rotary vibration excitation device. The exciting force of acoustic transmitter is approximately 10 N. The frequency of transmitted square pulse is set as 100 Hz, which amounts to the baud rate of 200 bit/s. A packet of 100-bit modulated square-wave binary sequence is sent at a time. Then the acoustic transmission performance is examined when the simulated drillstring is driven at a rotation speed of 0, 80, and 140 r/min in the experiment, respectively. Each transmission is performed for five times at every rotation speed for a certain modulation scheme. During the data transmission, an impact impulse signal, as shown in Figure 11, produced by a hammer is acted on the right end of simulated drillstring to artificially generate a downlink noise disturbing the uplink signal. The duration time of the impulse is nearly 0.5 ms. Figure 12 shows the BER curves of the transmitted ASK-, FSK-, and PSK-modulated data at different rotation speeds. The corresponding measured average bit error rates (BERs) at different rotation speeds are listed in Table 4.

Table 4: The measured average BER for three basic modes of modulation at different rotation speeds.

Rotation speed (r/min)	Modulation	Single receiver	Dual receiver
0	ASK	3.8%	2.2%
0	FSK	2.8%	2.0%
0	PSK	2.6%	1.6%
80	ASK	15.0%	5.2%
80	FSK	13.6%	3.8%
80	PSK	21.2%	8.2%
140	ASK	22.8%	8.6%
140	FSK	16.2%	6.2%
140	PSK	32.0%	12.2%

The experimental results demonstrate that the three modulation schemes have a similar average BER approximately in the range of 1.6%–3.8% for the single- and dual-receiver modes when the simulated drillstring does not rotate, but in general the PSK modulation is more superior to others. This verifies the validity of the aforementioned numerical simulation of BER performance. And the BER in the dual-receiver mode is slightly lower as shown in Figure 12(a). In other

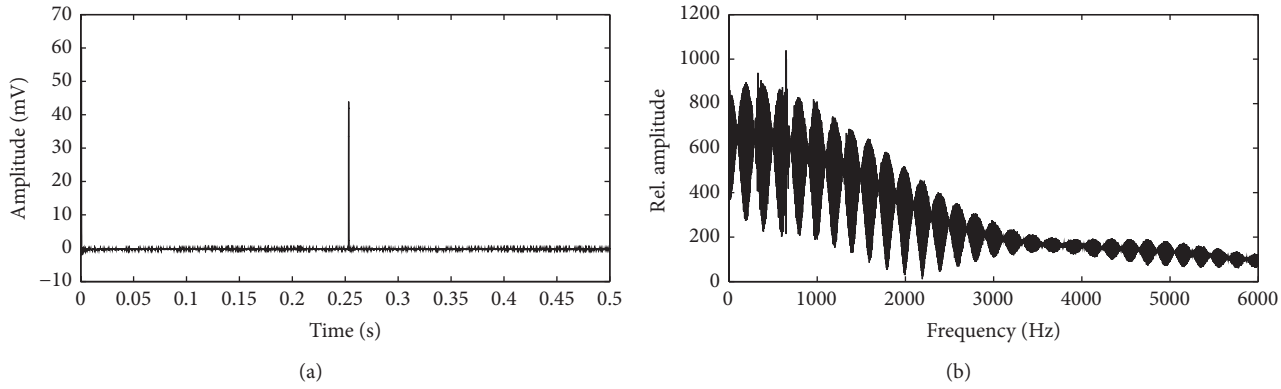

Figure 11: The disturbance pulse signal imposed by a hammer. (a) Time-domain signal, (b) frequency-domain signal.

words, the single-receiver mode is available for use under appropriate receiver positions and higher SNR conditions. However, as the rotation speed increases from 0 to 140 r/min, the acoustic transmission performance in the single-receiver mode becomes far worse as indicated in Figures 12(b) and 12(c). For example, as seen in Table 4, the average BER for the PSK modulation becomes much worse gradually from 2.6% to 21.2% and 32% at different rotation speeds, but a relatively low BER rising from 1.6% to 8.2% and 12.2% is achieved in the dual-receiver mode. Furthermore, the BER for the PSK modulation is inferior to that for the ASK modulation in the circumstance of rotating simulated drillstring because of the scatterings and the phase shifts of modulate waves resulting from mechanical vibrations. In contrast, the FSK modulation provides a better BER performance. Referring to Table 4, the average BER for the FSK modulation is nearly reduced by half as compared with that for the PSK modulation when the simulated drillstring rotates at the rotation speed of 80 r/min and 140 r/min in the single-receiver mode. However, when the dual-receiver mode is enabled, the corresponding BER for the FSK modulation declines sharply to 3.8% and 6.2% from 13.6% and 16.2%, respectively. In addition, the ASK modulation suffers from a higher BER slightly inferior to the FSK modulation for the dual-receiver prototype. It can be concluded that the PSK modulation is more adapted for the stable channel conditions because of the more sensitivity to phase noises, while the FSK modulation is an attractive modulation when the phase changes too quickly to be tracked. It is also indicated that, when properly implemented, a modified ASK, such as OOK (on-off keying) modulation with different protection time delays for the symbol "1" or "0," can actually exhibit a lower probability of error versus SNR by using two receivers, especially over a limited bandwidth channel.

As mentioned earlier, the transmission of acoustic telemetry data through drillstring itself has been periodically contemplated. Acoustic telemetry systems have been able to transmit data at rates up to 30 bit/s. A primary problematic issue related to acoustic transmission along drillstring during drilling operations is that the echo noise tends to reduce the SNR, regardless of the noise source. Consequently, the acoustic transmission rate and telemetry range are reduced because of the poor BER. In fact, vibration, in physics, is commonly an oscillatory motion. The discussed acoustic transmission performance is measured in the form of longitudinal vibration in the tube axis direction. From the performed experimental results, the echo noise is well cancelled by the proposed dual-receiver scheme with an improved average BER. As shown in Table 4, it is, respectively, reduced by 14.2%, 9.9%, and 19.8% for the ASK, FSK, and PSK modulations at the maximum rotation speed of 140 r/min. However, comparing with the BER simulation results as shown in Figure 6, the measured results represent a certain worse average probability of bit error. This phenomenon may result from coupled waves, which are mainly generated by the excitation axis deviation and the bending deflection of rotary simulated drillstring in the experiment. In practice, the axial, torsional, and lateral vibrations do not exist independently in rotary drilling. Among the couple modes, the coupled transverse mode is a major cause of drilling failures [24]. However, this mode conversion from extensional waves to bending waves accounts for extensional wave attenuation and distorted acoustic data signal [25]. The transmitted pulses tend to spread out because of interactions with the transmission medium, which leads to resonance effects and eventually produces an additional energy loss. Although the BER is still slightly high compared with the practical applications, the proposed dual-receiver method is simple to operate and available to allow the ringing to fall to a tolerable level. In particular, along with a proper combined intersymbol interference and optimized modulation coding scheme, such as MFSK (M-ary frequency-shift keying) or OFDM (orthogonal frequency division multiplexed) modulation, depending on the SNR and multipath fading intensity, it can achieve the effective suppression of echo interference with the improvement of data transmission performance in drillstring channel.

5. Conclusions

Acoustic telemetry is a promising technique to transmit the downhole information to the surface in a drilling operation. However, multiple-echo suppression is a more critical problem in the drillstring where echoes travel freely up and

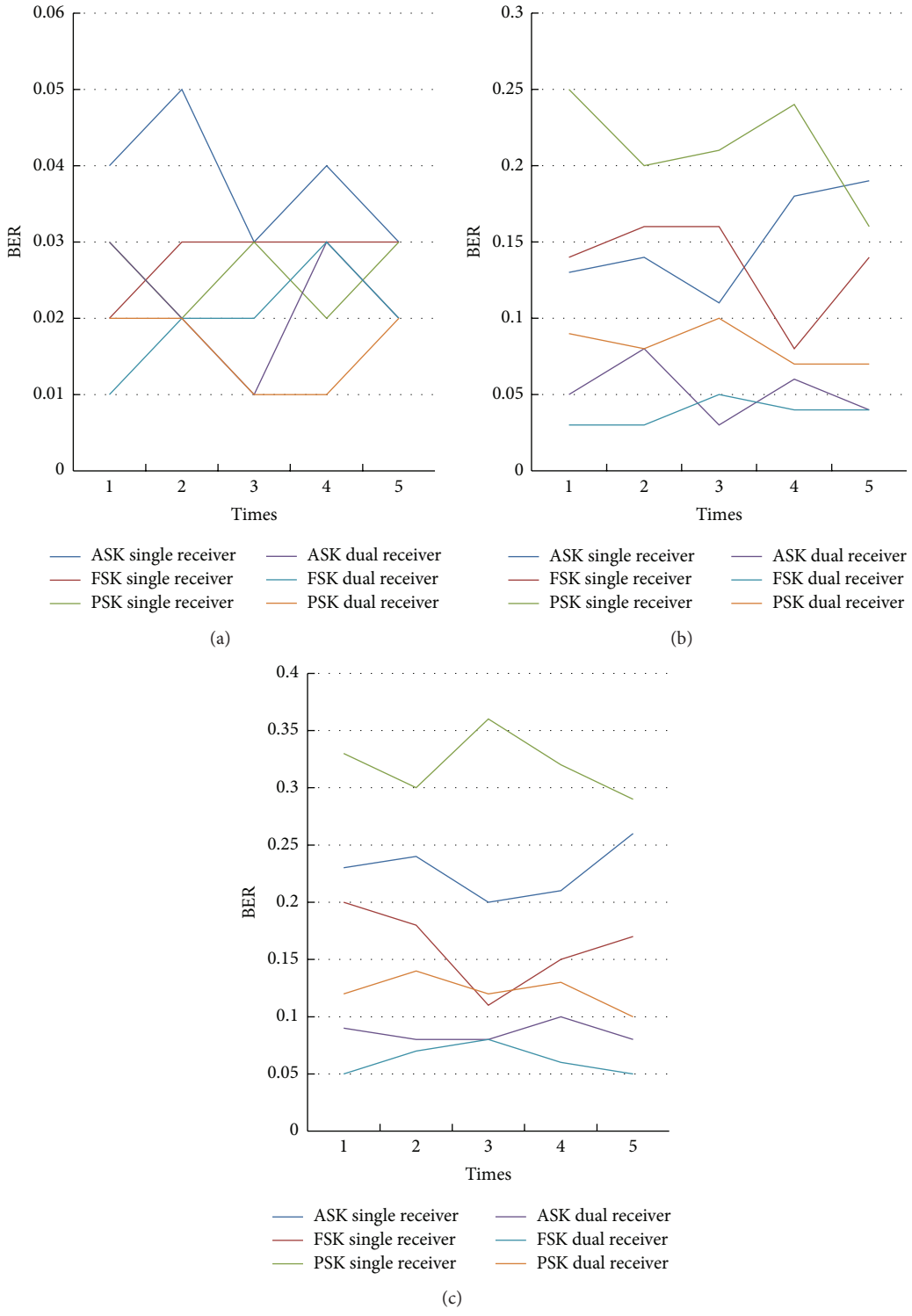

Figure 12: The measured BER curves of ASK-, FSK-, and PSK-modulated acoustic data at different rotation speeds. (a) 0, (b) 80 r/min, and (c) 140 r/min.

down the drillstring and confuse the transmission of data. Considering the fact that the dominant surface noise source and the uplink signal propagate in opposite directions, an improved simplified echo suppression technique using dual receivers is proposed by introducing the uplink and downlink channel responses. Acoustic transmission performances of ASK-, FSK-, and PSK-modulated signals in the periodic drillstring channel are simulated in single- and dual-receiver modes. Then the BER performances under different receiver modes and rotation speeds are tested by imposing the

dynamic vibration excitation on a rotary simulated drillstring. The experimental results show that the dual-receiver mode has a significant advantage over the single-receiver mode, especially under the condition of drillstring rotation. And the use of two spaced acoustic receivers with proper modulation scheme can offer a better SNR and further a greater data rate or distance in multipath channel of periodic drillstring.

Conflict of Interests

The authors declare that there is no conflict of interests regarding the publication of this paper.

Acknowledgments

The authors thank the National Natural Science Foundation of China (nos. 50905095, 61121003) and Changjiang Scholars and Innovative Research Team in University (IRT1203) for supporting this research.

References

[1] L. S. Kumar, W. K. Han, Y. L. Guan, S. Sun, and Y. H. Lee, "Optimal energy transfer pipe arrangement for acoustic drill string telemetry," *IEEE Transactions on Geoscience & Remote Sensing*, vol. 52, no. 11, pp. 6999–7007, 2014.

[2] C. Acar, A. Aljifri, Y. Bekkhouce, M. Maalej, I. Nwogbogu, and S. Vannuffelen, "Optimizing reservoir testing operations with downhole wireless telemetry system," in *Proceedings of the International Petroleum Technology Conference*, vol. 5, pp. 3666–3674, Doha, Qatar, January 2014.

[3] L. Cheng, T. Ding, and W. Peng, "An experimental rig for near-bit force measurement and drillstring acoustic transmission of BHA," *Measurement*, vol. 44, no. 4, pp. 642–652, 2011.

[4] L. Gao, D. Finley, W. Gardner et al., "Acoustic telemetry can deliver more real-time downhole data in underbalanced drilling operations," in *Proceedings of the IADC/SPE Drilling Conference—Achieving our Goals: People, Planning and Performance*, pp. 485–490, February 2006.

[5] D. McNeill, M. Reeves, M. Hernandez, L. Lawrence, B. Redmond, and R. Russell, "Intelligent' wired drill-pipe system allows operators to take full advantage of latest downhole sensor developments," in *Proceedings of the International Petroleum Technology Conference (IPTC '08)*, vol. 3, pp. 1659–1665, December 2008.

[6] V. V. Shah, W. R. Gardner, and D. G. Kyle, "Receiver for an acoustic telemetry system," US2008137481, 2008.

[7] G. S. Rosa, J. R. Bergmann, and S. R. Zang, "Electromagnetic analysis of wireless telemetry for oil fields," in *Proceedings of the 15th SBMO/IEEE MTT-S International Microwave and Optoelectronics Conference (IMOC '13)*, August 2013.

[8] D. S. Drumheller, "Acoustical properties of drill strings," *Journal of the Acoustical Society of America*, vol. 85, no. 3, pp. 1048–1064, 1989.

[9] M. E. Reeves, P. L. Camwell, and J. McRory, "High speed acoustic telemetry network enables real-time along string measurements, greatly reducing drilling risk," in *Proceedings of the Offshore Europe Oil and Gas Conference and Exhibition 2011*, vol. 2011, pp. 458–469, September 2011.

[10] O. Hoshuyama, "Dual-microphone echo canceller for suppressing loud nonlinear echo," in *Proceedings of the IEEE International Conference on Acoustics, Speech, and Signal Processing (ICASSP '12)*, pp. 181–184, March 2012.

[11] X. He, R. A. Goubran, and P. X. Liu, "A novel sub-band adaptive filtering for acoustic echo cancellation based on empirical mode decomposition algorithm," *International Journal of Speech Technology*, vol. 17, no. 1, pp. 37–42, 2014.

[12] M. Zhu, H. Wang, G. Chen, and K. Muto, "A two-stage adaptive algorithm in the frequency domain for a multichannel feedforward active noise control system," *International Journal of Acoustics and Vibrations*, vol. 18, no. 4, pp. 148–154, 2013.

[13] W. L. B. Jeannès, P. Scalart, G. Faucon, and C. Beaugeant, "Combined noise and echo reduction in hands-free systems: a survey," *IEEE Transactions on Speech and Audio Processing*, vol. 9, no. 8, pp. 808–820, 2001.

[14] J. W. Rector III and B. P. Marion, "The use of drill-bit energy as a downhole seismic source," *Geophysics*, vol. 56, no. 5, pp. 628–634, 1991.

[15] D. S. Drumheller and D. D. Scott, "Circuit for echo and noise suppression of acoustic signals transmitted through a drill string," US5274606, 1993.

[16] F. Poletto, "Use of dual waves for the elimination of reverberations in drill strings," *Journal of the Acoustical Society of America*, vol. 111, no. 1, pp. 37–40, 2002.

[17] S. Sinanović, D. H. Johnson, and W. R. Gardner, "Directional propagation cancellation for acoustic communication along the drill string," in *Proceedings of the IEEE International Conference on Acoustics, Speech and Signal Processing (ICASSP '06)*, vol. 4, pp. 521–524, May 2006.

[18] D. S. Drumheller, "Attenuation of sound waves in drill strings," *Journal of the Acoustical Society of America*, vol. 94, no. 4, pp. 2387–2396, 1993.

[19] T. G. Barnes and B. R. Kirkwood, "Passbands for acoustic transmission in an idealized drill string," *Journal of the Acoustical Society of America B*, vol. 51, no. 5, pp. 1606–1608, 1972.

[20] W. R. Gardner and V. V. Shah, "High data rate acoustic telemetry system," WO2001021928 A3, 2001.

[21] L. Cheng, C. Jinfeng, L. Zhao, F. Shangchun, and D. Tianhuai, "Characteristics analysis of joint acoustic echo and noise suppression in periodic drillstring waveguide," *Shock and Vibration*, vol. 2014, Article ID 741314, 10 pages, 2014.

[22] J. D. Oetting, "A comparison of modulated techniques for digital radio," *IEEE Transactions on Communication*, vol. 27, no. 12, pp. 1752–1762, 1979.

[23] D. S. Drumheller, "Wave impedances of drill strings and other periodic media," *Journal of the Acoustical Society of America*, vol. 112, no. 6, pp. 2527–2539, 2002.

[24] A. Ghasemloonia, D. Geoff Rideout, and S. D. Butt, "Analysis of multi-mode nonlinear coupled axial-transverse drillstring vibration in vibration assisted rotary drilling," *Journal of Petroleum Science and Engineering*, vol. 116, pp. 36–49, 2014.

[25] D. S. Drumheller, "Coupled extensional and bending motion in elastic waveguides," *Wave Motion*, vol. 17, no. 4, pp. 319–327, 1993.